RSC Advances

ROYAL SOCIETY OF CHEMISTRY

www.rsc.org/advances

Cite this: DOI: 10.1039/c0xx00000x

www.rsc.org/xxxxxx

ARTICLE TYPE

Tuning fluorescence of aggregates for end-functionalized polymers through varying polymer chains with different polarities

Pei-Yang Gu, You-Hao Zhang, Dong-Yun Chen, Cai-Jian Lu, Feng Zhou, Qing-Feng Xu* and Jian-Mei Lu*

Received (in XXX, XXX) Xth XXXXXXXXX 20XX, Accepted Xth XXXXXXXXX 20XX
DOI: 10.1039/b000000x

In the past several decades, a great attention has been focused on the control of light emission of luminescent materials. Compared to our previous work of an aggregation-induced emission (AIE) initiator, an aggregation-caused quenching (ACQ) initiator (TPP-A) has been successfully synthesized and acted as an initiator of atom transfer radical polymerization (ATRP). Four end-functionalized polymers, PS-A, PS-NI, PNIPAM-A and PNIPAM-NI, were obtained using TPP-A or TPP-NI as an initiator *via* ATRP, respectively. TPP-A exhibits a weak charge transfer (CT) and ACQ, but TPP-NI possesses a strong CT and AIE. After two initiators were introduced to polystyrene (PS) chains, the CT of PS-A and PS-NI are well-preserved, but their photoluminescence (PL) intensity is increased because the PS chains could separate initiators from intermolecular interactions and restrict their intramolecular rotations. However, the emission behaviours of PNIPAM-A is different from that of PS-A due to the high polarity of PNIPAM chain. When the temperature of solution for PNIPAM-A is above the lower critical solution temperature (LCST), the PNIPAM-A solution possessed higher emission intensities than those measured at room temperature due to decrease the polarity of PNIPAM chain and the emission behaviours of PNIPAM-NI are similar to that of PS-NI.

1 Introduction

Many efforts have been devoted to the development of luminescent materials with tunable optical properties due to their practical applications.[1-23] In the past several decades, a great of attention has been focused on the control of light emission of organic dyes in their dilute solutions. More recently, much work has been done to the manipulation of their optical properties in aggregate or solid state.[24-31] It is our interest to investigate whether it is possible to obtain an organic dye whose emission can be controlled in both solution and aggregate state. Among various kinds of potential organic dyes, 1,3,5-triarylpyrazoline has attracted growing attention due to their excellent optical properties.[32-40] As shown in Chart 1, two of the aryl rings in the 1- and 3- position communicate electronically through the pyrazoline-π-system. Therefore, the optical properties of pyrazoline can be adjusted with a suitable choice of the substituents in 1- or 3- position. Moreover, the optical properties of luminescent materials can be tailored not only by chemical modification of their structure but also by doping treatment. The organic dyes containing polymer film can be considered as a solid solution, in which an organic core is surrounded by polymer chains. The polarity of polystyrene (PS) chain is lower than that of poly(*N*-isopropylacrylamide) (PNIPAM) chain. As a result, PS chain can be considered as a lowly polar solid 'solvent', while PNIPAM chain can be considered as a highly polar solid 'solvent'. Tian and co-workers[23] reported two new series of amphiphilic copolymers which contained the segments of a monomeric aggregation-induced emission (AIE) fluorophore, *N*-(2-hydroxypropyl)methacrylamide, [2-(methacryloyloxy)ethyl]trimethylammoniumchloride, and/or 2,2,2-trifluoroethyl methacrylate (TFEMA). The higher quantum yields of copolymers can be obtained through increasing the molar fractions of the hydrophobic AIE fluorophores and/or the trifluoroethyl moieties. Using 1-mol% of AIE fluorophores with the tuning of molar fractions of TFEMA, 40% quantum yield was achieved, whereas only less than 10% quantum yield was obtained for the polymers without the TFEMA segments. Moreover, PNIPAM is a representative temperature-responsive polymer that exhibits a rapid and reversible hydration-dehydration change in response to small temperature cycles around its lower critical solution temperature (LCST = 32 ºC) in aqueous media, indicating that the polarity of PNIPAM is decreased in water when the temperature above LCST.[41-52] The detailed relationship between the hydration-dehydration changing PNIPAM chain and optical properties of end-functionalized PNIPAM may be of interest.

Our previous work introduced a single AIE unit (4-(1-(2-butyl-1,3-dioxo-2,3-dihydro-1H-benzo[de]isoquinolin-6-yl)-5-(4-(dimethylamino)phenyl)-4,5-dihydro-1H-pyrazol-3-yl)phenyl 2-bromo-2-methylpropanoate, abbreviated as TPP-NI) into a

polymer chain *via* atom transfer radical polymerization (ATRP).[53-55] The AIE property of end-functionalized polymers can be adjusted through polymer polarity. The polymer chain length and sterical hindrance may also affect the AIE property of end-functionalized polymers. Herein, TPP-NI end-functionalized PNIPAM, PNIPAM-NI, was obtained. The AIE property of PNIPAM-NI can be adjusted through varying temperature that leads to changing the polymer polarity, which avoided effect of the polymer chain length and sterical hindrance. We are also interested in how polymer chains affect the aggregation-caused quenching (ACQ) molecule emission. Whether is it possible to find a method to prevent ACQ-molecule from quenching in the aggregate state is important because polymer chains might weaken π–π stacking and intermolecular interaction, which could enhance the luminescence. Therefore, we designed and successfully synthesized an ACQ initiators, 4-(5-(4-(dimethylamino)phenyl)-1-phenyl-4,5-dihydro-1H-pyrazol-3-yl)phenyl 2-bromo-2-methylpropanoate (abbreviated as TPP-A) and introduced the initiator into polymer chains (PS or PNIPAM) *via* ATRP. In this work, we have systematically studied the effect of PS and PNIPAM chains on the two initiators.

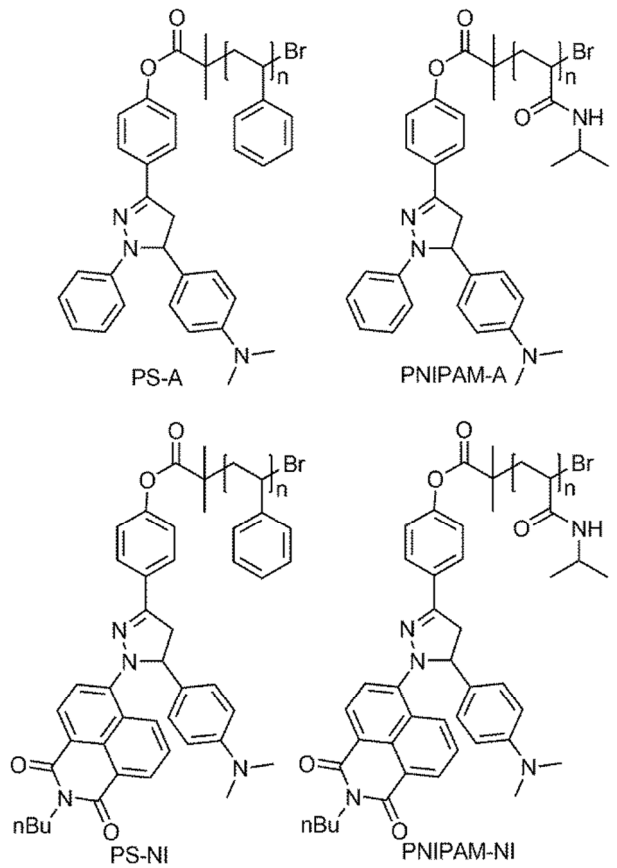

Chart 1 Structures of polymers.

2 Experimental section

2.1 Materials

N-Isopropylacrylamide (NIPAM, Sigma-Aldrich) was recrystallized twice from benzene/hexane (10: 1, v/v) prior to use; Copper bromide (CuBr, Sinopharm Chemical Reagent Co., Ltd) was purified in acetic acid, washed with methanol and dried under vacuum to afford a white powder. Tris(2-(dimethylamino)ethyl)amine (Me_6TREN, Alfa Aesar, A Johnson Matthey Company), *4'*-hydroxyacetophenone (Tokyo Chemical Industry Co., Ltd.) and *4*-dimethylaminobenzaldehyde (Tokyo Chemical Industry Co., Ltd.) were used as received without further purification. TPP-NI and PS-NI was synthesized according to our previous report.[53] All other reagents and solvents were analytic pure and were used as received without further purification.

2.2 Characterization

Using $CDCl_3$ or DMSO-d_6 as solvent and tetramethylsilane (TMS) as the internal standard, ^{1}H NMR and ^{13}C NMR spectra were measured on INOVA 300 or 400 MHz NMR spectrometer at ambient temperature. UV-vis absorption spectra were determined on a Shimadzu RF540 spectrophotometer. The emission and excitation spectra were carried out at room temperature through Edinburgh-920 fluorescence spectra photometer. The ground-state geometry of two initiators were optimized *via* the density functional theory (B3LYP) with the 6-31G* basis set using the Gaussian 03 program package. The fluorescent quantum yields (QYs) were determined using a calibrated integrating sphere. Molecular weights and the polydispersity (PDI) relative to PS were measured using Waters1515 GPC with *N,N*-dimethylformamide (DMF) as a mobile phase at a flow rate of 1 mL min^{-1} and with column temperature of 30 ºC.

2.3 Preparation of Nanoaggregates

Stock solutions of PNIPAM-A or PNIPAM-NI in tetrahydrofuran (THF) with a concentration of 50 μmol mL^{-1} were prepared. Aliquots (1 mL) of the stock solutions were transferred to 10 mL volumetric flasks. After adding appropriate amounts of THF, hexane or water was added dropwise under vigorous stirring to furnish 5 μmol mL^{-1} solutions with defined fractions of hexane or water (f_h or f_w = 0 – 90 vol %). The procedures of preparing of two initiators and two end-functionalized PS are the same as described above for the end-functionalized PNIPAM. Spectral measurements of the resultant solutions or aggregate suspensions were performed immediately.

2.4 Cloud points measurement

Cloud points (CP) of aqueous solutions of PNIPAM-A or PNIPAM-NI were measured by UV-vis spectroscopy. Transmittance of the solution was recorded with a photodidode connected to a computer. The sample, whose concentration in distilled water was 2 mg mL^{-1}, was poured into a 1 cm cell. The cell holder in the spectrophotometer was thermally controlled. The change in transmittance at 650 nm was monitored by heating the solution at a rate of 0.1 ˚C min^{-1}.

2.5 Synthesis

2.5.1 Synthesis of TPP-A

The synthesis of TPP-A (Scheme 1) was similar to the reported method to prepare TPP-NI.[53] The detailed characterizations were provided in supporting information.

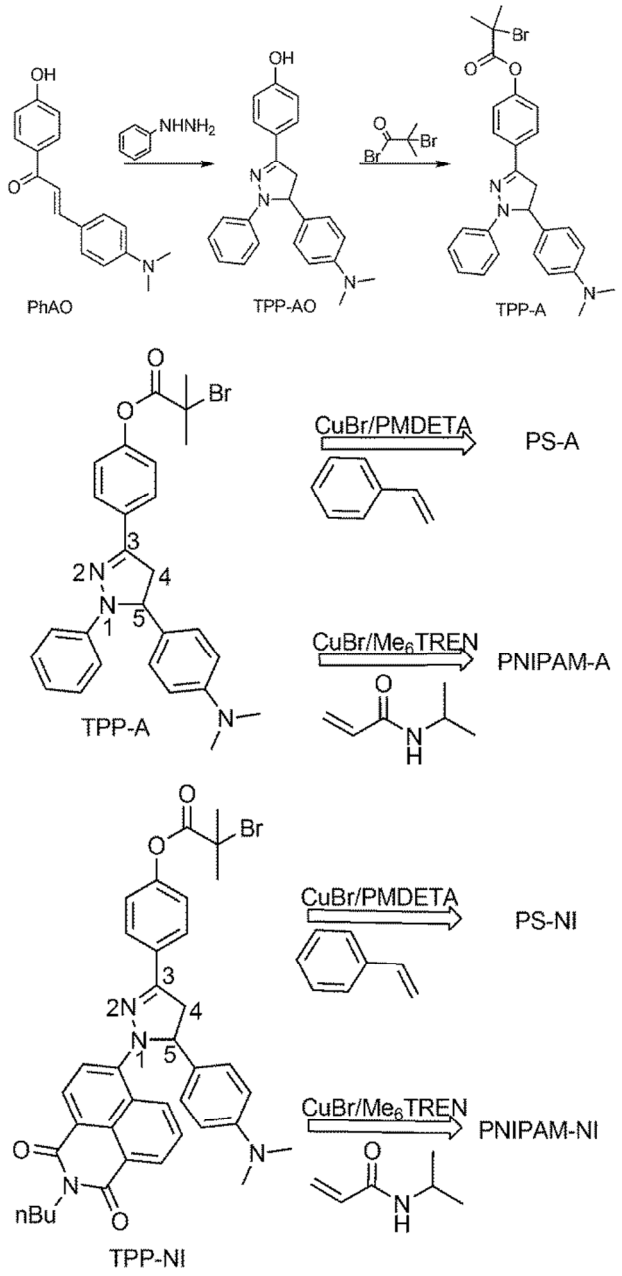

Scheme 1 Synthesis of TPP-A and polymers.

^{1}H NMR (400 MHz, DMSO-d_6) δ 7.86 – 7.80 (m, 2H), 7.27 – 7.21 (m, 2H), 7.14 (dd, J = 15.1, 7.9 Hz, 4H), 7.03 (dd, J = 6.3, 2.4 Hz, 2H), 6.71 (t, J = 7.2 Hz, 3H), 5.38 (dd, J = 12.1, 6.4 Hz, 1H), 3.87 (dd, J = 17.4, 12.1 Hz, 1H), 3.08 (dd, J = 17.4, 6.3 Hz, 1H), 2.86 (s, 6H), 2.07 (s, 6H).

^{13}C NMR (400 MHz, DMSO-d_6) δ 170.09, 150.88, 146.74, 144.71, 131.16, 129.25, 127.35, 127.13, 121.98, 118.97, 113.53, 63.44, 57.49, 43.48, 30.50.

HR-MS (m/z): $[M+H]^+$ Ion Formula: $C_{27}H_{29}BrN_3O_2$, Calcd for, 506.1364; Found, 506.1437.

2.5.2 Synthesis of PNIPAM-NI

The ATRP of NIPAM was performed at 50 ˚C in DMF. A typical polymerization was described as follows. NIPAM (1.13 g, 10 mmol), TPP-NI (6.80 mg, 0.01 mmol), CuBr (1.44 mg, 0.01 mmol), and Me_6TREN (2.3 mg, 0.01 mmol) were dissolved in DMF and the mixture was placed into a round-bottomed flask. The flask was sealed and cycled between vacuum and Argon three times. The polymerization was conducted at 50 ˚C for a certain time. The polymerization was stopped by quenching the flask in ice water. After being diluted with DMF, the diluted solution was passed through an alumina column to remove the copper catalyst, and the filtrate was precipitated by addition of ethyl ether. The precipitation was filtrated and dried under vacuum. The monomer conversion determined by gravimetry is 23%. The number-average molecular weight (M_n) was measured to be 26100 g mol^{-1} with M_w/M_n = 1.19 by GPC.

2.5.3 Synthesis of PS-A and PNIPAM-A

The synthesis of PS-A was similar to the reported method to prepare PS-NI, while PNIPAM-A was similar to the PNIPAM-NI.

3 Results and discussion

3.1 Calculation

The ground-state geometry of two initiators were optimized *via* the density functional theory (B3LYP) with 6-31G* basis set using the Gaussian 03 program package.[56-58] As shown in Figure 1a/b, the phenyl rings in the 3-position and 5-position of two initiators exhibit the similar dihedral angles. However, the phenyl ring in the 1-position of TPP-A exhibits the dihedral angle of 4°, indicating that the phenyl ring in the 1-position of TPP-A is almost coplanar with pyrazoline-π-system. When the sterical hindering group, NI, was introduced into the pyrazoline in 1-position, the dihedral angle of TPP-NI in the 1-position is increased from 4^o to 58^o.[53] The whole molecule of TPP-NI takes a non-planar configuration, which helps to impede the π-π stacking interaction to some extent in aggregate state, or at the film state. In addition, the spatial distributions of the highest occupied molecular orbital (HOMO) and the lowest unoccupied molecular orbital (LUMO) levels of two initiators were calculated and have been shown in Figure 1c/d/e/f. The electron density of TPP-A is changed a little between HOMO and LUMO orbits. However, the electron density distributions of the HOMO for TPP-NI mainly locate on pyrazoline ring and *N,N*-dimethylaniline group while the LUMO orbital is mainly distributed on NI group. Thus, a charge-transfer (CT) interaction can occur between the electron donor moieties and the electron acceptor moieties.

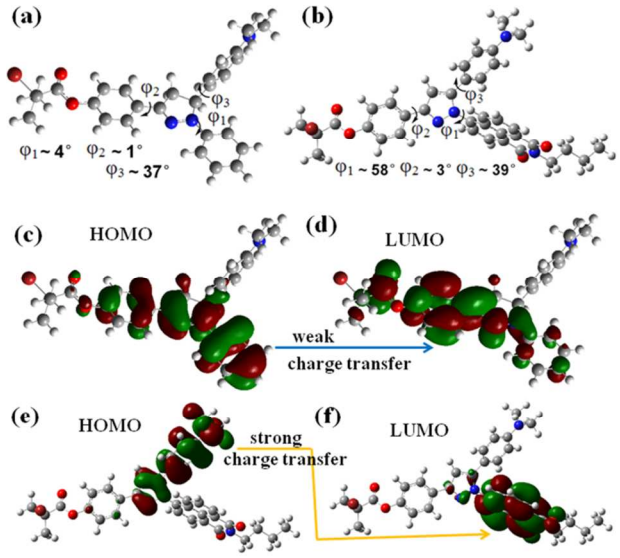

Figure 1 Optimized ground-state geometry of TPP-A (a) and TPP-NI (b) with B3LYP/6-31G* in the gas phase; calculated spatial distributions of the HOMO and LUMO levels of the TPP-A (c, d) and TPP-NI (e, f).

3.2 Solvent effect

The absorption and emission spectra of two initiators were measured in different polar solvents to elucidate the solvatochromism effect. As shown in Table 1 and Figure 2a, the absorption spectra of TPP-A in different solvents are similar with absorption band at 363 nm, which can be assigned to the π-π* transition involving an intramolecular charge transfer from the 1-Ph-N(1) donor to the Ar-C(3)=N(2) acceptor. TPP-A emits strong blue emission with maximum peak at 433 nm (λ_{ex} = 363 nm) in hexane, while the emission wavelength is only red-shifted 0.14 eV (23 nm) with the increase of solvent polarity from hexane to DMF. These results indicate that TPP-A exhibits weak CT effect. TPP-NI shows multiple absorption bands at 330 nm, 437 nm and 461 nm, which may be deduced to the π–π* transition and CT from *N,N*-dimethylaniline to NI, respectively. The absorption wavelength of TPP-NI is red-shifted 0.23 eV (38 nm), while the solvent changes from non-polar hexane to polar DMF. Moreover, the emission wavelength was also red-shifted 0.32 eV (69 nm), while the solvent polarity was increased from hexane to DMF. These phenomena indicate that TPP-NI exhibits strong CT effect. When the polarity of the solvent increased, charge transfer states of TPP-NI can be more stabilized in polar media such as DMF due to the highly polarized nature of the charge transfer state, and the PL intensity is decreased. As can be seen from Table S4, the percent of the shortest lifetime is increased with increasing the solvent polarity.

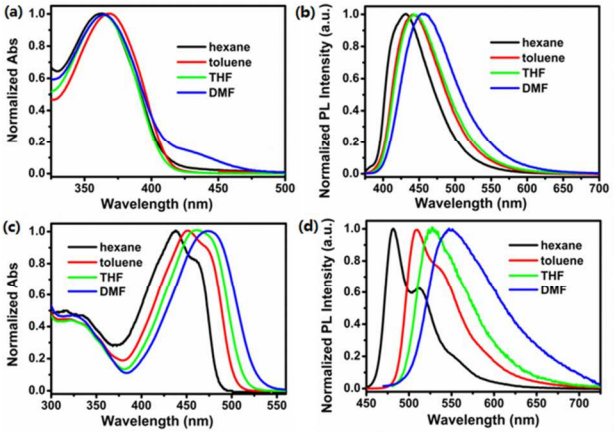

Figure 2 Normalized absorption and emission spectra of TPP-A (a, b) and TPP-NI (c, d) in different solvents (λ_{ex} = λ_{abs}, respectively, Concentration: 25 μmol L^{-1})

Table 1 Photophysical data for TPP-A and TPP-NI

	TPP-A			TPP-NI		
State	λ_{abs} [a]	λ_{em} [b]	QY[c]	λ_{abs}	λ_{em}	QY
Hexane	363	433	46.7	437, 461	480, 510	29.4
Toluene	365	442	34.6	451	507, 535	20.9
THF	363	444	38.8	460	525	2.30
DMF	363	456	43.3	475	549	n. d.[f]
DMF/water[d]	363	478	1.77	469	562	1.0

[a] The absorption wavelength (nm). [b] The emission wavelength (nm). [c] Fluorescence quantum yield (%). [d] DMF/water = 1: 9, by volume. [f] not determined

As shown in Table2/3 and Figure S19/20/22/23, the absorption and emission spectra of two initiators' end-functionalized polymers in different polar solvents were measured to confirm the preservation of CT in polymers. The absorption and emission patterns of four end-functionalized polymers were similar to those of their initiators, indicating that CT effect was well-preserved.

3.3 Aggregates fluorescence

To investigate their aggregation behaviours, the absorption and emission spectra of two initiators in DMF/water mixtures with different water fractions were measured and shown in Figure S18 and Figure 3. With the increase of the f_w from 0 to 90 %, the PL intensity of TPP-A is decreased and the emission wavelength is red-shifted. The effect of f_w on TPP-NI is different from that on TPP-A according to our previous work.[53] When the f_w is 60 %, the PL intensity of TPP-NI reaches a maximum value and the emission wavelength changes a little. The different fluorescent behaviours of two initiators are due to the different conformation of two initiators. Generally, aggregation will force the dye inside the nanoaggregates to pack more densely; therefore, it may be obvious that a more crowded environment will force the inside dyes to adopt a more coplanar geometry. According to calculation, the phenyl ring in the 1-position of TPP-A is almost coplanar with pyrazoline-π-system. By contrast, the whole molecule of TPP-NI takes a non-planar configuration; therefore, the configuration of TPP-A may be more coplanar geometry in aggregate state that leads to the emission intensity quenched and emission wavelength red-shifted, while it is difficult for TPP-NI to form coplanar geometry due to the poor coplanarity of TPP-NI.

Moreover, the interactions between TPP-NI molecules are smaller that of TPP-A molecules due to the sterical hindrance in TPP-NI, which reduces excitonic interactions as well as polarizability effects.[59]

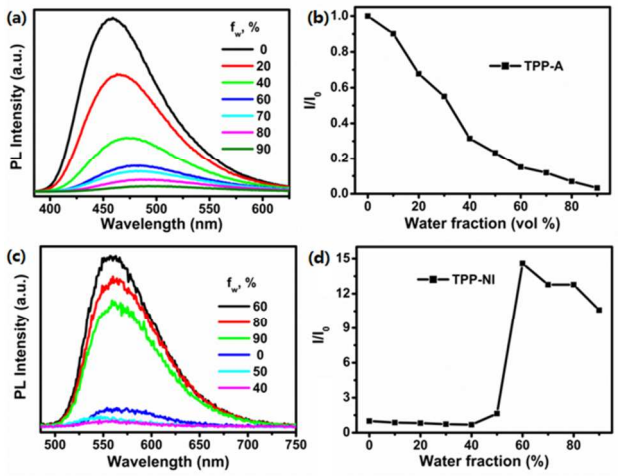

Figure 3 Emission spectra of TPP-A (a) and TPP-NI (c) with the composition of the DMF/water mixture; Change in the relative PL intensity (I/I_0) of TPP-A (b) and TPP-NI (d) in the DMF/water mixture. I_0 = PL intensity in DMF solution. Concentration: 25 μmol L^{-1}; excitation wavelength: 363 and 467 nm, respectively.

The emission behaviours of PS-A and PS-NI were studied using DMF/ethanol mixture. The absorption and emission spectra of PS-A in aggregate state were shown in Figure S21 and Figure 4, the emission intensity is increased and the emission wavelength is blue-shifted with the ethanol fraction (f_e) increasing. The optical behaviors of PS-NI are similar to those of PS-A in aggregate state.[53] The polarity of PS chains is low. The PS chains can be used as building blocks to reduce the intermolecular interaction between initiators, and hence eliminate the aggregation quenching effect and amplify the aggregation emission. On the other hand, for microenviroment of initiator, the dyes were surrounding by solvents only, but for microenviroment of end-functionalized polymers, the dyes were surrounding by solvents and polymer chains.

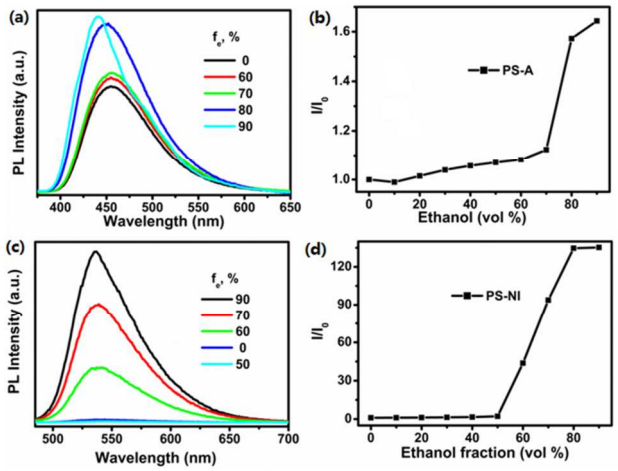

Figure 4 Emission spectra of PS-A (a) and PS-NI (c) with the composition of the DMF/ethanol mixture; Change in the relative PL intensity (I/I_0) of TPP-A (b) and TPP-NI (d) in the DMF/ethanol mixture. I_0 = PL intensity in DMF solution. Concentration: 5 μmol L^{-1}; excitation wavelength: 365 and 475 nm, respectively.

Table 2 Photophysical data for PS-A and PS-NI

	PS-A			PS-NI		
State	λ_{abs} [a]	λ_{em} [b]	QY[c]	λ_{abs}	λ_{em}	QY
Toluene	365	440	60.4	463	508	26.8
THF	365	442	62.2	463	526	3.68
DMF	365	457	61.6	475	539	0.05
DMF/ethanol[d]	369	440	65.7	489	537	14.7

[a] The absorption wavelength (nm). [b] The emission wavelength (nm). [c] Fluorescence quantum yield (%). [d] DMF/ethanol = 1: 9, by volume.

PNIPAM exhibits solubility in THF, DMF and water, and poor solubility in hexane, while two initiators exhibit solubility in hexane, THF and DMF, and poor solubility in water. To investigate the aggregation behaviours of PNIPAM-A and PNIPAM-NI, their absorption and emission spectra in aggregate state were studied in two different mixture systems (THF/hexane and THF/water). The traces of PL intensity depending on f_h in the THF/hexane mixtures for PNIPAM-A are shown in Figure 5. With increasing f_h from 0 to 50%, the PL intensity is increased a little and the emission wavelength is blue-shifted which could be ascribed to CT effect due to the low polarity of hexane. When a "large" amount of hexane ($f_h \geq 60$ %) is added into THF, the PL intensity is decreased due to forming the nanoparticles. When the f_h is as high as 60 %, the light scattering effect of the nanoparticles could be observed in Figure S24. There are at least two factors which affect the emission of TPP-A: (1) when hexane is added into THF, the polarity of the mixture is decreased and this is beneficial to emission; (2) when a "large" amount of hexane is added, the nanoparticles are formed which are not beneficial to emission because the aggregation behaviour of PNIPAN-A is similar to those of TPP-A due to the different polarity of NIPAM and TPP-A. Those results are confirmed by the aggregation behaviour of PNIPAM-A in THF/water. The PL intensity is decreased with increasing f_w due to the high polarity of water. On the basis of chemical intuition, PNIPAM-A should self-assemble into micelle in THF/hexane or THF/water solution due to the different solubility between PNIPAM and TPP-A. Possible self-assembling processes are proposed in Scheme 2. TPP-A cores are surrounded by PNIPAM chains in THF/water solution because TPP-A cannot dissolve in water. By contrast, PNIPAM chains are surrounded by TPP-A in THF/hexane solution because PNIPAM cannot dissolve in hexane. In the above two cases, polymer chains are difficult to reduce the intermolecular interactions and restrict intramolecular rotation. Thus, the emission behaviour of PNIPAM-A is similar to that of TPP-A.

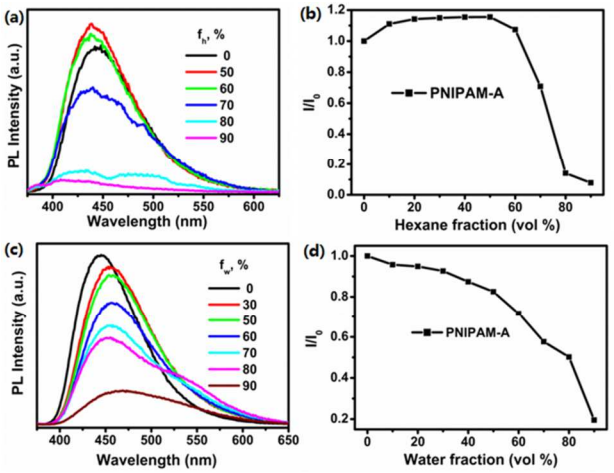

Figure 5 Emission spectra of PNIPAM-A with the composition of the THF/hexane (a) and THF/water (c) mixture; Change in the relative PL intensity (I/I_0) of PNIPAM-A in the THF/hexane (b) and THF/water (d) mixture. I_0 = PL intensity in DMF solution. Concentration: 5 μmol L^{-1}; excitation wavelength: 365 nm.

Table 3 Photophysical data for PNIPAM-A and PNIPAM-NI

	PNIPAM-A			PNIPAM-NI		
State	λ_{abs} [a]	λ_{em} [b]	QY[c]	λ_{abs}	λ_{em}	QY
THF	365	442	38.9	466	529	2.5
DMF	366	456	48.7	471	544	n. d.[f]
THF/hexane[d]	366	431	21.4	463	538	12.1
THF/water[e]	367	464	14.5	465	533	9.80

[a] The absorption wavelength (nm). [b] The emission wavelength (nm).[c] Fluorescence quantum yield (%). [d] THF/hexane = 1: 9 for PNIPAM-A 1: 7 for PNIPAM-NI, by volume. [e] THF/water = 1: 9, by volume. [f] not determined

The emission behaviours of PNIPAM-NI in THF/hexane and THF/water mixture are different from those of PNIPAM-A, but they are similar to those of TPP-NI. The PL intensity of PNIPAM-NI is enhanced with increasing f_h because of the low polarity of hexane. Even though a "large" amount of hexane is added into the solution of PNIPAM-NI in THF, the PL intensity is still increased because TPP-NI is noncoplanar molecule. When water was added into the solution of PNIPAM-NI in THF, firstly, the PL intensity is decreased due to the high polarity of water; secondly, the PL intensity is increased due to formation the nanoparticles. Those phenomena are similar to that of TPP-NI in DMF/water mixture.

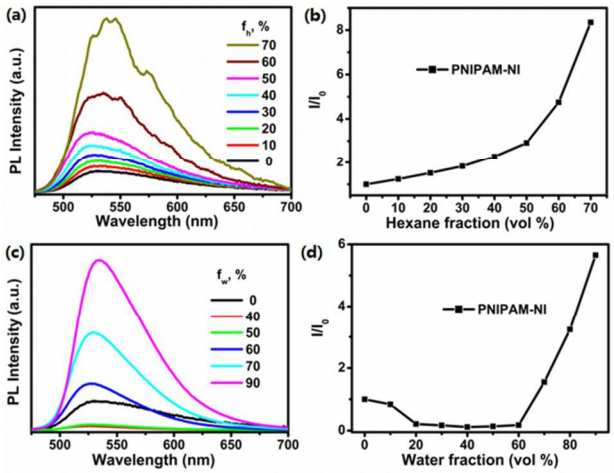

Figure 6 Emission spectra of PNIPAM-NI with the composition of the THF/hexane (a) and THF/water (c) mixture; Change in the relative PL intensity (I/I0) of PNIPAM-A in the THF/hexane (b) and THF/water (d) mixture. I0 = PL intensity in DMF solution. Concentration: 5 μmol L^{-1}; excitation wavelength: 475 nm.

3.4 LCST of PNIPAM

PNIPAM-A gave a clear solution in cold water, which became turbid by raising the temperature. To determine the LCST for the liquid/solid phase transition, the transmittance (%) of an aqueous PNIPAM-A solution (2 mg m L^{-1}) was measure using UV–vis absorption spectroscopy upon raising the temperature at the heating rate of 0.1 ˚C min^{-1}. Figure 7a/c shows the transmittance versus temperature plots (cloud point curves). We used 50% transmittance points as the LCST. The LCST of the PNIPAM-A in aqueous solution was 31.6 ˚C. The result of the temperature-dependent the hydrodynamic diameter was agreement with the temperature-dependent optical transmittance. We used the same method to measure the LCST of the PNIPAM-NI which is 32.8 ^{o}C.

The fluorescence spectra of the aqueous PNIPAM-A and PNIPAM-NI solutions at room temperature (25 ° C) and at 40 ° C (>LCST) are examined in Figure 7b/d. The emission intensity at 40 °C is comparatively higher than their respective counterparts at room temperature because polymer chains can be used as building blocks to reduce the intermolecular interaction between initiators.

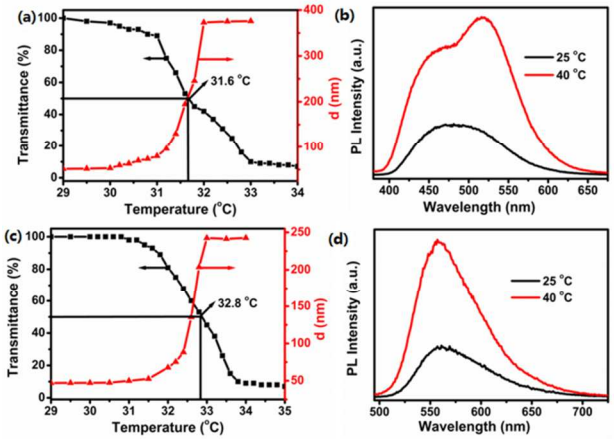

Figure 7 Effects of temperature on transmittance and particle size for the aqueous PNIPAM-A (a) and PNIPAM-NI (c) solutions (2 mg mL^{-1}); Emission spectra of the aqueous PNIPAM-A (b) and PNIPANM-NI (d) solutions at room temperature and at 40 °C (2 mg mL^{-1}, excitation wavelength 363 and 475 nm, respectively).

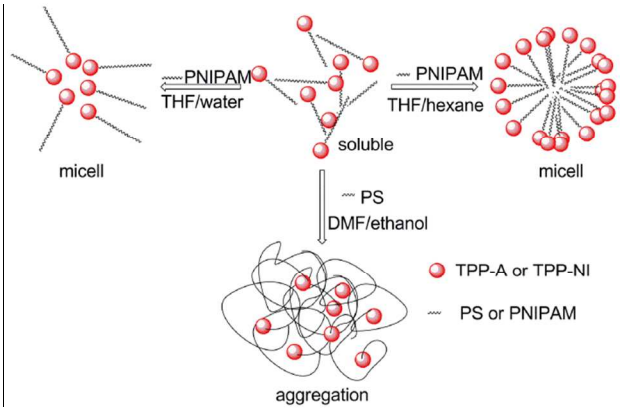

Scheme 2 Schematic illustrations of aggregate states for four polymers.

Conclusion

In this work, four end-functionalized polymers, PS-A, PS-NI, PNIPAM-A and PNIPAM-NI, were obtained using TPP-A or TPP-NI as an initiator *via* ATRP. TPP-A exhibits a weak CT and ACQ, but TPP-NI possesses a strong CT and AIE. After initiators were introduced to PS chains, the CT of PS-A and PS-NI are well-preserved, while their PL intensity is increased because the PS chains could separate initiators from intermolecular interactions and restrict their intramolecular rotations. However, the emission behaviours of their end-functionalized PNIPAM (PNIPAM-A and PNIPAM-NI) are different, but the emission behaviours of PNIPAM-A and PNIPAM-NI are similar to their corresponding initiators, respectively. As a result, PNIPAM-A exhibits a weak CT and ACQ and PNIPAM-NI exhibits a strong CT and AIE due to the different polarity of PNIPAM and initiators. The LCST of the aqueous PNIPAM-A and PNIPAM-NI solutions were 31.6 and 32.8 °C, respectively. At 40 °C, polymer aqueous solution possessed higher emission intensities than those measured at room temperature. In summary, we have successfully utilized the polymer chains to tune the optical properties of luminophores, and studied the interaction between polymer chains and initiators with different CT.

Acknowledgements

The authors graciously thank the Chinese Natural Science Foundation (21071105, 21371128 and 51228302), the Specialized Research Fund for the Doctoral Program of Higher Education of China (grant no. 20113201130003) and SUN-WIN joint Project.

Notes and references

College of Chemistry, Chemical Engineering and Materials Science, Collaborative Innovation Center of Suzhou Nano Science and Technology, Soochow University, Suzhou 215123, China. Fax: +86 512 65880367; Tel: +86 512 65880368; E-mail: lujm@suda.edu.cn, xuqingfeng@suda.edu.cn

† Electronic Supplementary Information (ESI) available: [details of experimental section]. See DOI: 10.1039/b000000x/

1 T. H. Kim and T. M. Swager, *Angew. Chem. Int. Ed.*, 2003, **42**, 4803.
2 Q. Li, Y. He, J. Chang, L. Wang, H. Chen, Y. W. Tan, H. Wang and Z. Shao, *J. Am. Chem. Soc.*, 2013, **135**, 14924.
3 C. H. Lee, H. J. Yoon, J. S. Shim and W. D. Jang, *Chem. Eur. J.*, 2012, **18**, 4513.
4 B. L. Ma, F. Zeng, X. Z. Li and S. Z. Wu, *Chem. Commun.*, 2012, **48**, 6007.
5 P. Y. Gu, Y. H. Zhang, G. Y. Liu, J. F. Ge, Q. F. Xu, Q. Zhang and J. M. Lu, *Chem. Asian J.*, 2013, **8**, 2161.
6 P. N. H. Huynh, R. R. Walvoord and M. C. Kozlowski, *J. Am. Chem. Soc.*, 2012, **134**, 15621.
7 L. Y. Niu, Y. S. Guan, Y. Z. Chen, L. Z. Wu, C. H. Tung and Q. Z. Yang, *J. Am. Chem. Soc.*, 2012, **134**, 18928.
8 Y. Ooyama and Y. Harima, *J. Mater. Chem.*, 2011, **21**, 8372.
9 Y. Qian, J. Karpus, O Kabil, S. Y. Zhang, H. L. Zhu, R. Banerjee, J. Zhao and C. He, *Nature Commun.*, 2011, **2**, 495.
10 M. Pawlicki, H. A. Collins, R. G. Denning and H. L. Anderson, *Angew. Chem. Int. Ed.*, 2009, **48**, 3244.
11 X. J. Lu, L. F. Zhang, L. Z. Meng and Y. H. Liu, *Polym. Bull.*, 2007, **59**, 195.
12 S. Uchiyama, N. Kawai, A. P. Silva and K. Iwai, *J. Am. Chem. Soc.*, 2004, **126**, 3032.
13 X. L. Luo, J. N. Li, C. H. Li, L. P. Heng, Y. Q. Dong, Z. P. Liu, Z. S. Bo and B. Z. Tang, *Adv. Mater.*, 2011, **23**, 3261.
14 Q. Zhang, D. H. Qu, X. Ma and H. Tian, *Chem. Commun.*, 2013, **49**, 9800.
15 S. S. Pennadam, M. D. Lavigne, C. F. Dutta, K. Firman, D. Mernagh, D. C. Gorecki and C. Alexander, *J. Am. Chem. Soc.*, 2004, **126**, 13208.
16 M. Teng, X. Jia, X. Chen, Z. Ma and Y. Wei, *Chem. Commun.*, 2011, **47**, 6078.
17 D. Ross, M. Gaitan and L. E. Locascio, *Anal. Chem.*, 2001, **73**, 4117.
18 S. Uchiyama, Y. Matsumura, A. P. Silva and K. Iwai, *Anal. Chem.*, 2004, **76**, 1793.
19 G. Zhang, S. E. Kooi, J. N. Demas and C. L. Fraser, *Adv. Mater.*, 2008, **20**, 2099.
20 S. Uchiyama, Y. Matsumura, A. P. Silva and K. Iwai, *Anal. Chem.*, 2003, **75**, 5926.
21 G. A. Baker, S. N. Baker and T. M. Mccleskey, *Chem. Commun.*, 2003, 2932.
22 A. Seeboth, J. Kriwanek and R. Vetter, *J. Mater. Chem.*, 1999, **9**, 2277.
23 H. Lu, F. Su, Q. Mei, Y. Tian,W. Tian, R. H. Johnson and D. R. Meldrum, *J. Mater. Chem.*, 2012, **22**, 9890.
24 X. Qi, H. Li, J. W. Y. Lam, X. Yuan, J. Wei, B. Z. Tang and H. Zhang, *Adv. Mater.*, 2012, **24**, 4191.
25 C. Tan, X. Qi, X. Huang, J. Yang, B. Zheng, Z. An, R. Chen, J. Wei, B. Z. Tang, W. Huang and H. Zhang, *Adv. Mater.*, 2014, **26**, 1735.
26 A. Patra and U. Scherf, *Chem. Eur. J.*, 2012, **18**, 10074.
27 T. He, X. Tao, J. Yang, D. Guo, H. Xia, J. Jia and M. Jiang, *Chem. Commun.*, 2011, **47**, 2907.
28 Y. Liu, Z. Wang, G. Zhang, W. Zhang, D. Zhang and X. Jiang, *Analyst*, 2012, **137**, 4654.
29 Y. Hong, L. Meng, S. Chen, C. W. T. Leung, L. T. Da, M. Faisal, D. A. Silva, J. Liu, J. W. Y. Lam, X. Huang and B. Z. Tang, *J. Am. Chem.Soc.*, 2012, **134**, 1680.
30 Z. Shi, J. Davies, S. H. Jang, W. Kaminsky and A. K. Y. Jen, *Chem. Commun.*, 2012, **48**, 7880.
31 F. Wang, J. Wen, L. Huang, J. Huang and J. Ouyang, *Chem. Commun.*, 2012, **48**, 7395.
32 C. J. Fahrni, L. C. Yang and D. G. VanDerveer, *J. Am. Chem. Soc.*, 2003, **125**, 3799.
33 J. Cody, S. Mandal, L. C. Yang and C. Fahrni, *J. Am. Chem. Soc.*, 2008, **130**, 13023.
34 P. Y. Gu, C. J. Lu, Q. F. Xu, G. J. Ye, W. Q. Chen, X. M. Duan, L. H. Wang and J. M. Lu, *J. Polym. Sci., Part A: Polym. Chem.*, 2012, **50**, 480.
35 T. Sano, Y. Nishio, Y. Hamada, H. Takahashi, T. Usuki and K.Shibata, *J. Mater. Chem.*, 2000, **10**, 157.
36 E. Palaska, D. Erol and R. Demirdamar, *Eur. J. Med. Chem.*, 1996, **31**, 43.
37 J. Barberá, K. Clays, R. Giménez, S. Houbrechts, A. Persoons and J. L.Serrano, *J. Mater. Chem.*, 1998, **8**, 1725.
38 P. L. Zhao, F. Wang, M. Z. Zhang, Z. M. Li, W. Huang and G. F.Yang, *J. Agric. Food Chem.*, 2008, **56**, 10767.
39 P. Banerjee, S. Pramanik, A. Sarkar and S. C. Bhattacharya, *J. Phys. Chem. B*, 2009, **113**, 11429.

40 D. Xiao, L. Xi, W. Yang, H. Fu, Z. Shuai, Y. Fang and J. Yao, *J. Am. Chem. Soc.*, 2003, **125**, 6740.
41 T. Matsuda, Y. Saito and K. Shoda, *Biomacromolecules*, 2007, **8**, 2345.
42 J. Yip and J. Duhamel, *Macromolecules*, 2011, **44**, 5363.
43 X. Z. Zhang, R. X. Zhuo, J. Z. Cui and J. T. Zhang, *Int. J. Pharm.*, 2002, **235**, 43.
44 Y. Shiraishi, R. Miyamoto, X. Zhang and T. Hirai, *Org. Lett.*, 2007, **9**, 3921.
45 K. Fujimoto, C. Iwasaki, C. Arai, M. Kuwako and E. Yasugi, *Biomacromolecules*, 2000, **1**, 515.
46 Z. G. Gao, X. D. Tao, Y. Cui, T. Kakuchi and Q. Duan, *Polym. Chem.*, 2011, **2**, 2590.
47 X. D. Tao, Z. G. Gao, T. Satoh, Y. Cui, T. Kakuchi and Q. Duan, *Polym. Chem.*, 2011, **2**, 2068.
48 Q. Duan, Y. Miura, A. Narumi, X. Shen, S. Sato, T. Satoh and T. Kakuchi, *J. Polym. Sci. Part A: Polym. Chem.*, 2006, **44**, 1117.
49 G. Zhou, I. I. Harruna, W. L. Zhou, W. K. Aicher and K. E. Geckeler, *Chem. Eur. J.*, 2007, **13**, 569.
50 L. Tang, J. K. Jin, A. J. Qin, W. Z. Yuan, Y. Mao, J. Mei, J. Z. Sun and B. Z. Tang, *Chem. Commun.*, 2009, 4974.
51 C. T. Lai, R. H. Chien, S. W. Kuo and J. L. Hong, *Macromolecules*, 2011, **44**, 6546.
52 Y. W. Lai, S. W. Kuo and J. L. Hong, *RSC Adv.*, 2012, **2**, 8194.
53 P. Y. Gu, C. J. Lu, F. L. Ye, J. F. Ge, Q. F. Xu, Z. J. Hu, N. J. Li and J. M. Lu, *Chem. Commun.*, 2012, **48**, 10234.
54 J. Qiu and K. Matyjaszewski, *Macromolecules*, 1997, **30**, 5643.
55 J. Ueda, M. Atsuyaman, M. Kamigaito and M. Sawamoto, *Macromolecules*, 1998, **31**, 557.
56 S. Kim, Q. Zheng, G. S. He, D. J. Bharali, H. E. Pudavar, A. Baev and P. N. Prasad, *Adv. Funct. Mater.*, 2006, **16**, 2317.
57 P.-Y. Gu, C.-J. Lu, Z.-J. Hu, N.-J. Li, T.-T. Zhao, Q.-F. Xu, Q.-H. Xu, J.-D. Zhang and J.-M. Lu, *J. Mater. Chem. C*, 2013, **1**, 2599.
58 Y. Zhang, J. Sun, G. Bian, Y. Chen, M. Ouyang, B. Hu and C. Zhang, *Photochem. Photobiol. Sci.*, 2012, **11**, 1414.
59 Y.-S. Huang, J. Gierschner, J. P. Schmidtke, R. H. Friend and D. Beljonne, *Phys. Rev. B*, 2011, **84**, 205311.